

Received July 11, 2019, accepted July 29, 2019, date of publication August 1, 2019, date of current version August 16, 2019.

Digital Object Identifier 10.1109/ACCESS.2019.2932625

# Time-Coordinated Control for Unmanned Aerial Vehicle Swarm Cooperative Attack on Ground-Moving Target

YUEQI HOU<sup>1</sup>, XIAOLONG LIANG<sup>1,2</sup>, LYULONG HE<sup>1,2</sup>, AND JIAQIANG ZHANG<sup>1</sup>

<sup>1</sup>National Key Laboratory of Air Traffic Collision Prevention, Air Force Engineering University, Xi'an 710051, China

<sup>2</sup>Shaanxi Province Laboratory of Meta-Synthesis for Electronic and Information System, Xi'an 710051, China

Corresponding author: Xiaolong Liang (afeu\_lxl@sina.com)

This work was supported by the National Natural Science Foundation of China under Grant 61703427.

**ABSTRACT** In this paper, cooperative attack control law analysis and design problems for unmanned aerial vehicle (UAV) swarm attack on ground-moving target with time-coordinated strategies are investigated. First, the time-coordinated control problem for a single UAV is formulated, which is the foundation of solving the problem of a single UAV arriving at the desired attack position relative to ground-moving target at a specific terminal time. Then, relative motion between each UAV and ground-moving target is considered as a finite-time time-varying tracking system problem, and the difference between expected output and system output is defined as tracking error vector. The control law is obtained by linear quadratic optimal control theory to minimize the energy cost in the whole process and the tracking error at the terminal time. Besides, time-coordinated function, which is critical to coordinate terminal time among all UAVs in the UAV swarm, is proposed to model time-coordinated strategies. Finally, numerical simulations show that the proposed control law can steer UAV swarm to arrive at the desired attack positions and achieve the time-coordinated strategies effectively.

**INDEX TERMS** UAV swarm, time-coordinated control, cooperative attack, ground-moving target, linear quadratic optimal control.

## I. INTRODUCTION

Through efficient coordination, UAV swarm which is composed of many UAVs connected by communication network, can emerge much better performance than several independent individuals [1]. Cooperative executing missions of UAV swarm without constant supervision of human operators has attracted increasingly attention in both civil and military applications. For the case of attacking a ground target, UAV swarm must execute a coordinated maneuver to arrive at the predefined positions over the target from multiple angles simultaneously [2]. Time-coordinated strategies in these missions are effective to achieve the maximum reward by saturation attack and improve the overall abilities of UAV swarm. In general, time-coordinated control problems have been investigated in various applications, including

multi-agents [3]–[5], multiple underwater vehicles [6], multi-UAVs [7]–[10] and multi-missiles [11]–[13]. Compared with robots, UAVs move in three-dimensional space with positive speed restrictions and can not stop or back off. Compared with missiles, UAVs can change the velocity within its allowable range, or increase the flight time by hovering.

Over the past decades, the cooperative-timing attack issues for multi-UAVs system have been extensively investigated, and tremendous achievements have been scored in variety of regions. For the case of attacking ground stationary targets, there are two main ways to achieve time-coordination. One way is to coordinate the velocity and path of each UAV. In order to achieve cooperative-timing planning problems among teams of UAV involving simultaneous arrival, tight sequencing, and loose sequencing, a cooperative control strategy based on coordination functions and coordination variables is proposed in [8]. But there must be one of the UAVs flying at its maximum velocity. In [14], optimal cooperative

The associate editor coordinating the review of this manuscript and approving it for publication was Juan Liu.

time is designed as Estimated Time until Arrival (ETA) and cooperation function is solved by the ACO algorithm. Then, path and speed of each UAV can be computed according to ETA. Simple example of applying the consensus algorithm to the simultaneous arrival of multi-UAVs is given in [15]. This method assumes that the path planning has been completed and the simultaneous arrival is guaranteed only by coordinating the velocity of each UAV. Another way is to coordinate length of each UAV's path, where UAV's velocity can be a constant. To satisfy the UAV kinematic constraints in an obstacle environment and realize the simultaneous attacks, a distributed cooperative particle swarm optimization algorithm is developed to generate flyable and safe Pythagorean hodograph curve trajectories to achieve simultaneous arrival [16]. Suresh and Ghose [2], [17] present UAV grouping and coordination tactics for attacking a ground stationary target guarded by a layered defense network. The UAVs mission is to simultaneously attack the stationary target at specified attack angles, where the munitions' path is modeled as Dubins paths.

The methods proposed in [8], [14]–[17] are path pre-planning before cooperative attack, which are only suitable for static target attacks. Although there are few papers in the literature that investigate cooperative-timing attack of ground-moving target, there are several papers that have addressed different related applications using UAVs, such as multi-UAVs cooperative tracking of ground moving targets [18], [19], and multi-UAVs formation control with time constraints [9], [10]. Actually, cooperative attack on ground-moving targets can be considered as a formation control problem or optimal tracking problem [20] with terminal time constraint. There are a lot of researches in the literature that address formation control problems [21] or interconnected systems stabilization problems [22], [23] based on consistency theory. However, these methods can just achieve the desired formation within a finite time or fixed time, rather than in a specific terminal time. Multi-UAVs formation control with terminal constraints on position and velocity is addressed in [9]. A virtual leader is proposed to define the formation position of each UAV as the relative desired position and velocity with respect to the leader, which are considered as the terminal constraints. The control laws are obtained as the state feedback solution of a linear quadratic optimal control problem, and they are possible to make all vehicles join the formation concurrently at a specified time. The same problem is addressed in a three-dimensional space [10], and the control law is designed using the Lyapunov function. Considering the ground-moving target as a virtual leader, the above methods [9], [10] can be used to address the time-coordinated attack problem.

Motivated by above discussions, this paper focuses on how to control each UAV in the UAV swarm to reach the desired attack position at a specified terminal time when the target is moving. Compared with reference [14]–[16], the target in this paper is a moving in real time, and the motion of the target is uncertain. Consequently, path pre-planning or coordinating

the speed of each UAV are not suitable for this problem. In order to take target's motion into consideration, relative motion between each UAV and ground-moving target are modeled as a finite-time time-varying tracking system problem. Its core idea is that tracking error converges to zero at the terminal time. Compared with the existing time-coordinated control methods based on consistency theory, the proposed method can assign a specific arrival time for each UAV rather than all UAVs. Significantly, by this newly proposed approach, the terminal time and arrival position of each UAV are decoupled and various, which brings more possibilities for a variety of missions. The main contributions of this paper are summarized as follows: (i) Considering relative motion between each UAV and ground-moving target as a finite-time time-varying tracking system problem, the control law is obtained by optimal control theory. (ii) The Desired Attack Position (DAP) and time-coordinated function are defined to model the coordination of time and space. (iii) The time-coordinated strategies of simultaneous arrival within one group and interval arrival between groups are adopted to verify the validity and accuracy of the proposed control law.

The rest of this paper is organized as follows. The problem formulation is illustrated in Section II. In Section III, the cooperative attack control laws for a single UAV and UAV swarm are designed respectively. Simulation studies are given in Section IV. Finally, conclusions and future researches are presented in Section V.

## II. PRELIMINARIES

In this section, the models of the UAV and the ground-moving target are firstly described. A feedback linearization technique is then employed to simplify the UAV model to a double-integrator model. The time-coordinated attacking problem will be investigated based on the reduced model.

### A. KINEMATIC AND DYNAMIC MODELS OF UAV

In this paper, the UAV refers to a small fixed-wing UAV with an autopilot, and point-mass aircraft model [21] is used to describe its motion. In what follows, the dynamic model assumes that the UAV always performs coordinated maneuvers and the thrust is directed along the velocity vector. Suppose that there are  $n$  ( $n > 1$ ) UAVs with the same dynamic characteristics moving in  $R^3$ , which compose UAV swarm. In the inertial reference frame, the UAV kinematic equations can be described as follows

$$\begin{aligned}\dot{x}_i &= V_i \cos \gamma_i \cos \psi_i, \\ \dot{y}_i &= V_i \cos \gamma_i \sin \psi_i, \\ \dot{z}_i &= V_i \sin \gamma_i,\end{aligned}\quad (1)$$

where  $i = 1, \dots, n$  is the label of each UAV in UAV swarm.  $x_i, y_i$  denote the east and north displacement, respectively.  $z_i$  is altitude,  $V_i$  is the velocity,  $\gamma_i$  is the flight path angle and  $\psi_i$  is the heading angle, as shown in Fig. 1.

The corresponding dynamic equations are given by

$$\dot{V}_i = \frac{T_{hi} - D_{gi}}{m_i} - g_a \sin \gamma_i,$$

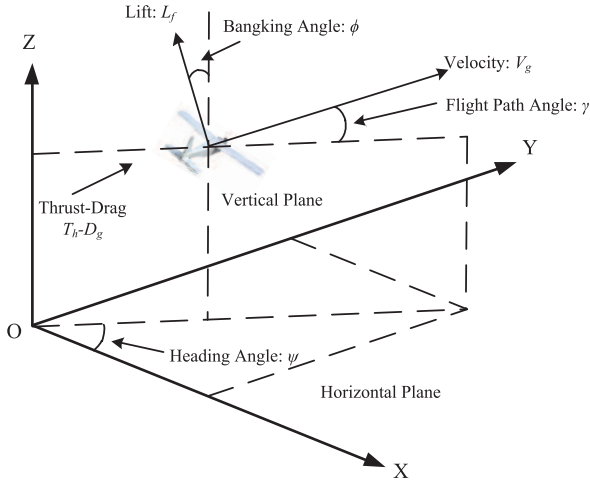


FIGURE 1. UAV model.

$$\begin{aligned} \dot{\gamma}_i &= \frac{g_a}{V_i} (n_{gi} \cos \phi_i - \cos \gamma_i), \\ \dot{\psi}_i &= \frac{L_{fi} \sin \phi_i}{m_i V_i \cos \gamma_i}, \end{aligned} \quad (2)$$

where  $m_i$  is the mass,  $D_{gi}$  is the drag,  $g_a$  is the gravitational acceleration,  $L_{fi}$  is the lift force. The control variables of the UAVs are the engine thrust  $T_{hi}$  controlled by the throttle, the g-load  $n_{gi} = L_{fi}/(m_i g_a)$  controlled by the elevator, and the banking angle  $\phi_i$  controlled by the combination of rudder and ailerons. Throughout the process of time-coordinated attacking, all the control variables should be constrained within the limits.

$$\begin{aligned} n_{g \min} &\leq n_{gi} \leq n_{g \max}, \\ T_{hi} &\leq T_{h \max}, \\ |\phi_i| &\leq \phi_{\max}. \end{aligned} \quad (3)$$

Based on the feedback linearization, the complicated nonlinear UAV model can be transformed into a linear time-invariant double-integrator model [21], [24], [25]. Specifically, we can differentiate the kinematic (1) once with respect to time, and then substitute the dynamic (2) to obtain

$$\ddot{x}_{ui} = a_{uxi}, \quad \ddot{y}_{ui} = a_{uyi}, \quad \ddot{z}_{ui} = a_{uzi}, \quad (4)$$

where  $a_{uxi}$ ,  $a_{uyi}$  and  $a_{uzi}$  are the certain control variables in the double-integrator model, which have the relationships with the actual control variables as follows

$$\begin{aligned} \phi_i &= \tan^{-1} \left[ \frac{a_{uyi} \cos \psi_i - a_{uxi} \sin \psi_i}{\cos \kappa_i - \sin \varepsilon_i} \right], \\ n_{gi} &= \frac{\cos \kappa_i - \sin \varepsilon_i}{g_a \cos \phi_i}, \\ T_{hi} &= [\sin \kappa + \cos \varepsilon_i] m_i + D_{gi}, \end{aligned} \quad (5)$$

where  $\kappa_i = \gamma_i(a_{uzi} + g_a)$ ,  $\varepsilon_i = \gamma_i(a_{uxi} \cos \psi_i + a_{uyi} \sin \psi_i)$ . The heading angle  $\psi_i$  and flight path angle  $\gamma_i$  are computed by

$$\tan \psi_i = \frac{\dot{y}_{ui}}{\dot{x}_{ui}}, \quad \sin \gamma_i = \frac{\dot{z}_{ui}}{V_{gi}}. \quad (6)$$

These actual control variables above are sent to the autopilot in real time, which automatically calculates the engine thrust and the rotation angles of rudder, ailerons and elevator.

*Remark 1:* A control law  $\mathbf{a}_{ui} = (a_{uxi}, a_{uyi}, a_{uzi})$  is designed in the following section. Then based on (4), (5) and (6), the actual control variables  $\phi_i$ ,  $n_{gi}$  and  $T_{hi}$  can be derived. Using the computed control variables  $(\phi_i, n_{gi}, T_{hi})$  in 3-DOF nonlinear UAV model, i.e. (1) and (2), multiple UAVs can achieve time-coordinated control.

### B. MODEL OF GROUND-MOVING TARGET

The ground-moving target in this paper refers to relatively slow target such as vehicle or ship whose speed is less than the maximum speed of the UAV. Compared with UAV, altitude change of the target on the ground or sea surface can be neglected. Therefore, it is also assumed that the target moves in a two-dimensional plane, regardless of the height fluctuations during motion, i.e.  $v_{tz} = 0$ . Target's state vector is

$$\mathbf{X}_t(k) = [x_t(k), v_{tx}(k), y_t(k), v_{ty}(k)]^T, \quad (7)$$

where  $x_t(k)$ ,  $y_t(k)$  and  $v_{tx}(k)$ ,  $v_{ty}(k)$  are the Cartesian coordinates of position and velocity of the target in the inertial reference frame, respectively. The equation of target's motion can be expressed as

$$\mathbf{X}_t(k+1) = f_t(\mathbf{X}_t(k)), \quad (8)$$

where  $f_t(\cdot)$  is the transformation function of target state. As discussed, the target trajectory is composed of a set of modes. In order to simulate the process of the target motion, CV, CA and CT models [26] are adopted here, and the process noise is negligible. The three models above are convenient to describe the movement process of the target and they are consistent with the movement of vehicles.

Constant Velocity (CV) Mode:

$$\mathbf{X}_t(k+1) = \begin{bmatrix} 1 & T & 0 & 0 \\ 0 & 1 & 0 & 0 \\ 0 & 0 & 1 & T \\ 0 & 0 & 0 & 1 \end{bmatrix} \mathbf{X}_t(k), \quad (9)$$

where  $T$  is the sampling time.

Constant Acceleration (CA) Mode:

$$\mathbf{X}_t(k+1) = \begin{bmatrix} 1 & T & 0 & 0 \\ 0 & 1 & 0 & 0 \\ 0 & 0 & 1 & T \\ 0 & 0 & 0 & 1 \end{bmatrix} \mathbf{X}_t(k) + \begin{bmatrix} \frac{T^2}{2} & 0 \\ T & 0 \\ 0 & \frac{T^2}{2} \\ 0 & T \end{bmatrix} \mathbf{a}_t(k), \quad (10)$$

where  $\mathbf{a}_t(k) = [a_{tx}(k), a_{ty}(k)]^T$  is the acceleration of target.

Coordinated Turn (CT) Mode:

$$\mathbf{X}_t(k+1) = \begin{bmatrix} 1 & \frac{\sin \omega T}{\omega} & 0 & -\frac{1 - \cos \omega T}{\omega} \\ 0 & \cos \omega T & 0 & -\sin \omega T \\ 0 & \frac{1 - \cos \omega T}{\omega} & 1 & \frac{\sin \omega T}{\omega} \\ 0 & \sin \omega T & 0 & \cos \omega T \end{bmatrix} \mathbf{X}_t(k), \quad (11)$$

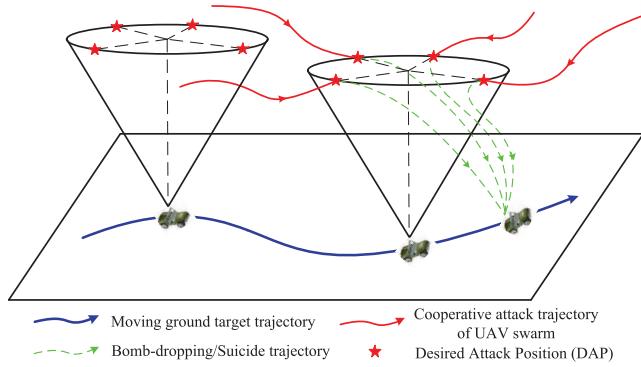


**FIGURE 2.** Mission scenario of UAV swarm attacking ground moving target simultaneously.

where  $\omega$  is the turn rate of the target of which sign determines the turning direction. If the target turns clockwise,  $\omega$  is negative. Based on the above three models, the process of the ground target’s motion can be completely described. Note that the control law proposed in following sections is not only applicable to targets modeled by CV, CA and CT, but also to targets with any other motion models.

**C. PROBLEM STATEMENT**

In the scenario,  $n$  UAVs are assigned to attack the ground-moving target cooperatively. Time-coordinated strategies such as simultaneous arrival or interval arrival are effective for improving suddenness or persistence of the attack. Simultaneous arrival strategy requires  $n$  UAVs to reach their predetermined Desired Attack Positions (DAP) at their terminal arrival times respectively, as shown in Fig. 2.

Not only is there a certain requirement on UAV’s relative position to target in the terminal time, but the relative velocity and entry angle should also be a specific range when UAV reaches the DAP. Denote the terminal relative position and velocity as

$$\mathbf{X}_{DAP} = [x_a, v_{ax}, y_a, v_{ay}, z_a, v_{az}]^T, \quad (12)$$

where  $x_a, y_a, z_a$  and  $v_{ax}, v_{ay}, v_{az}$  are the Cartesian coordinates of terminal relative position and velocity between UAV and target in the inertial reference frame, respectively. In what follows,  $\mathbf{X}_{DAP}$  is the terminal state constraint of the control system while designing time-coordinated attack control law.

UAV swarm is divided into several attack subgroups. According to the different roles in the mission, UAVs in UAV swarm can be divided into three types: commander UAV, subgroup leader and subgroup members, as shown in Fig. 3. The process of initiating and assigning cooperative attack tasks is as follows. After the commander UAV receives the attack task, the terminal arrival time  $t_f$  and desired attack position  $\mathbf{X}_{DAP}$  of each subgroup are coordinated on the basis of the attack modes, target characteristics, subgroup distribution, and so on. Then, the commander UAV assigns attack tasks to each subgroup, and sends attack parameters to the subgroup

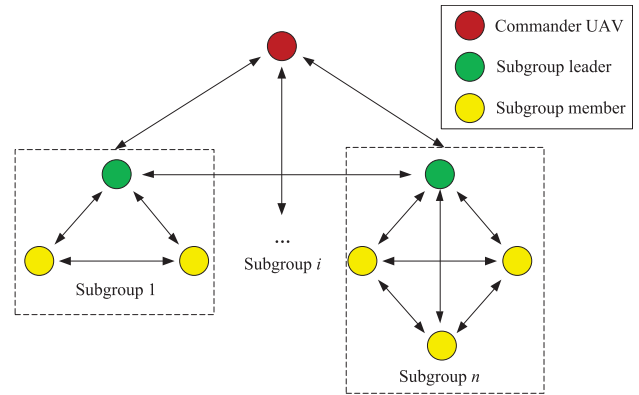


**FIGURE 3.** Coordinated control structure of UAV swarm.

leaders through the communication network. Finally, the subgroup leaders coordinate every subgroup member to set attack parameters and launch cooperative attack. By the way, the desired attack position is calculated by the commander UAV, which is not preprogrammed in a rigid position. Actually, there is some algorithm computing the optimal desired attack position, but this is not the focus of this paper.

After arriving at the DAPs, the attack modes are various from different types of UAVs. For a bomb-dropping UAV, the attack mode is to launch missiles or drop bombs. For a suicide UAV, the attack mode is to guide itself to the target by the guidance of the seeker and to explode once hitting the target. This paper focuses on how to control UAV swarm to reach their DAPs with the respective expected arrival time. Attack guidance (green curves in Fig. 2) intervals of each UAV can be negligible. Therefore, the interval time of attacking target can be approximately equal to the interval time of reaching DAP.

**III. COOPERATIVE ATTACK CONTROL LAW**

**A. CONTROL LAW FOR A SINGLE UAV**

In order to establish conveniently the mathematical model of the target, the target is regarded as an object moving in two-dimensional plane in Section II. However, in the process of deriving the control law, the target refers to an object moving in three-dimensional space for the sake of integrity of the theory. Fig. 4 is given to illustrate the scenario, where the point U, T and A represent the UAV, the target and the DAP, respectively. All of these points are moving in three-dimensional space, and the relative position between A and T remains fixed. It is assumed that there is a target tracking system to locate the target’s position and estimate its motion state. Hence, target’s position  $\mathbf{r}_t = [x_t, y_t, z_t]^T$ , velocity  $\mathbf{v}_t = [v_{tx}, v_{ty}, v_{tz}]^T$ , and acceleration  $\mathbf{a}_t = [a_{tx}, a_{ty}, a_{tz}]^T$  are known in real time. Denote UAV’s position, velocity and acceleration in the inertial reference frame as  $\mathbf{r}_u = [x_u, y_u, z_u]^T$ ,  $\mathbf{v}_u = [v_{ux}, v_{uy}, v_{uz}]^T$ , and  $\mathbf{a}_u = [a_{ux}, a_{uy}, a_{uz}]^T$ , respectively.

Relative position, velocity and acceleration between UAV and target can be described as

$$[\mathbf{r}, \mathbf{v}, \mathbf{a}]^T = [\mathbf{r}_u, \mathbf{v}_u, \mathbf{a}_u]^T - [\mathbf{r}_t, \mathbf{v}_t, \mathbf{a}_t]^T. \quad (13)$$

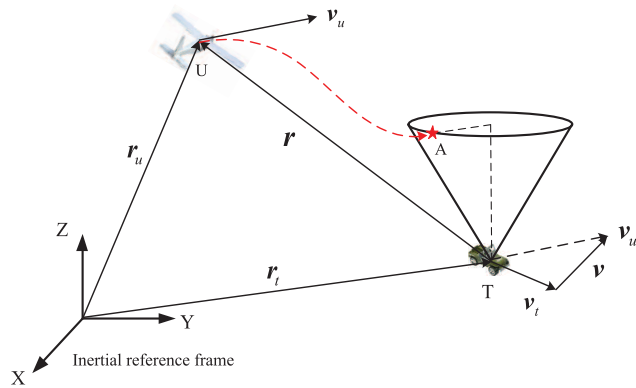


FIGURE 4. Relative motion between UAV and target.

The motion equation of UAV (4) and target (8-11) satisfies the property of second-order integrator. So the relative motion satisfies

$$\begin{aligned} \dot{r} &= \dot{r}_u - \dot{r}_t = v_u - v_t = v, \\ \dot{v} &= \dot{v}_u - \dot{v}_t = a_u - a_t = a. \end{aligned} \quad (14)$$

Let the  $r, v, a$  be respectively

$$\begin{aligned} r &= [x, y, z]^T, \\ v &= [v_x, v_y, v_z]^T = [\dot{x}, \dot{y}, \dot{z}]^T, \\ a &= [a_x, a_y, a_z]^T = [\dot{v}_x, \dot{v}_y, \dot{v}_z]^T. \end{aligned} \quad (15)$$

The relative motion model between UAV and target is regarded as a linear time-invariant system whose state space equation can be expressed as

$$\begin{aligned} \dot{X} &= AX + BU, \\ Y &= CX, \end{aligned} \quad (16)$$

where  $X = [x, v_x, y, v_y, z, v_z]^T$  is the system state,  $U = [a_x, a_y, a_z]^T$  is the system input.

$$A = I_3 \otimes \begin{bmatrix} 0 & 1 \\ 0 & 0 \end{bmatrix}, \quad B = I_3 \otimes \begin{bmatrix} 0 \\ 1 \end{bmatrix}, \quad C = I_6. \quad (17)$$

Let  $Y_d(t)$  denote the expected output vector and define the error vector

$$e(t) = Y_d(t) - Y(t) = Y_d(t) - X(t). \quad (18)$$

The error vector  $e(t)$  represents the difference between the system state and the expected output. In the scenario of time-coordinated attacking of UAV swarm, the desired relative position and velocity between UAV and target are only reached at the terminal time  $t_f$ , not in the whole process. Hence, the value of  $Y_d(t)$  at the terminal time is set to  $X_{DAP}$ :

$$Y_d(t_f) = X_{DAP}. \quad (19)$$

At the terminal time  $t_f$ , if Euclidean norm of error vector  $\|e(t_f)\|$  can be reduced to zero, the system state  $X(t_f)$  is close

to  $X_{DAP}$ . Considering the following linear quadratic optimal control problem, the quadratic cost function is chosen to be

$$J = \frac{1}{2} e^T(t_f) F e(t_f) + \frac{1}{2} \int_{t_0}^{t_f} U^T(t) R(t) U(t) dt, \quad (20)$$

where  $t_0$  and  $t_f$  represent the initial time and the terminal time, respectively.  $F$  is a non-negative symmetric constant matrix, which means the error weight matrix

$$F = \text{diag}(f_1, f_2, \dots, f_6) \geq 0. \quad (21)$$

Consider a time-varying weighting [9], [27] given by

$$R(t) = 1/t_{go}^N, \quad N \geq 0, \quad (22)$$

where the time to go is defined by

$$t_{go} \triangleq t_f - t. \quad (23)$$

For  $N = 0$ , the integral term in (20) becomes a pure energy-optimal control term. For  $N \geq 1$ , the cost becomes increasingly expensive so that the control eventually approaches to  $0$  at  $t = t_f$ . Introducing (22), we can conveniently shape the command profile by choosing proper  $N$ .

The first term in (20) is the terminal term, indicating the tracking error at  $t_f$ , that is, the sum of squared errors between  $X(t_f)$  and  $Y_d(t_f)$ . The second term in (20) is the process term that represents the magnitude of energy consumption during system control. The physical meaning of (20) is to optimize the energy consumption of the system during the control process and the system steady-state error at the terminal time. In other words, UAV's fuel consumption in the process of reaching the DAP and the error between UAV's state and DAP at the terminal time are comprehensive minimum.

Since the equation of system state given in (16-17) and the terminal constrains in (19) are decouple between the X-axis, Y-axis and Z-axis, optimal control law  $a_x^*$ ,  $a_y^*$  and  $a_z^*$  can be independently obtained. Therefore, the analysis and the solution of the optimal control law will be limited only to the X-axis. The system along X-axis is simplified to

$$A = \begin{bmatrix} 0 & 1 \\ 0 & 0 \end{bmatrix}, \quad B = \begin{bmatrix} 0 \\ 1 \end{bmatrix}, \quad C = I_2. \quad (24)$$

System state and system input are given by

$$X(t) = [x(t), v_x(t)]^T, \quad U(t) = a_x(t). \quad (25)$$

Let error weight matrix in (20)  $F = \text{diag}(f_1, f_2)$ , where  $f_1$  and  $f_2$  are the error weight of position and velocity, respectively. For the finite-time time-varying tracking system problem above, there is a unique optimal control. The state feedback solution of this optimal control problem is given by [28]

$$U^*(t) = -R^{-1}(t) B^T [P(t) X(t) - g(t)], \quad (26)$$

where  $P(t)$  is non-negative symmetric matrix, which is the unique solution of the following Riccati equation and its terminal constraint

$$\begin{aligned} -\dot{P} &= PA + A^T P - PBR^{-1}B^T P, \\ P(t_f) &= C^T(t_f) F C(t_f) = F. \end{aligned} \quad (27)$$

$\mathbf{g}(t)$  is a adjoint vector satisfying the following vector differential equation and its terminal constraint

$$-\dot{\mathbf{g}} = \left[ \mathbf{A} - \mathbf{B}\mathbf{R}^{-1}\mathbf{B}^T\mathbf{P} \right] \mathbf{g},$$

$$\mathbf{g}(t_f) = \mathbf{C}^T(t_f)\mathbf{F}\mathbf{Y}_d(t_f) = \mathbf{F}\mathbf{Y}_d(t_f). \quad (28)$$

In general, the solution of Riccati differential equation has no explicit expression, and can only be obtained by numerical algorithm. Runge-Kutta method is a high precision one-step algorithm widely used in engineering to solve this equation, including the famous Euler method. Euler method is the first-order form of Runge-Kutta method and its error is  $O(h)$ , where  $h$  is the time step. Due to the large accumulation of errors in the calculation process, Euler method is not adopted in practical application. One of the various Runge-Kutta methods is so common that it is often called fourth-order Runge-Kutta (RK4). RK4 is a fourth-order method and the error of each step is  $O(h^5)$ , and the total accumulated error is  $O(h^4)$ . Therefore, RK4 is great enough to meet the requirements of solving time and precision in practical applications.

Accordingly, RK4 is used to solve (27) and (28) here. Substituting  $\mathbf{A}$ ,  $\mathbf{B}$  and  $R(t)$  into (27) and assuming

$$\mathbf{P} = \begin{bmatrix} p_1 & p_2 \\ p_2 & p_3 \end{bmatrix}, \quad (29)$$

yields

$$\begin{aligned} \dot{p}_1 &= t_{go}^N p_2^2, \\ \dot{p}_2 &= -p_1 + t_{go}^N p_2 p_3, \\ \dot{p}_3 &= -2p_2 + t_{go}^N p_3^2, \end{aligned} \quad (30)$$

whose terminal constraint is given by

$$p_1(t_f) = f_1, \quad p_2(t_f) = 0, \quad p_3(t_f) = f_2. \quad (31)$$

Equation (30) is solved from  $t_f$  to  $t_0$ , where  $t_f$  is the initial time and  $t_0$  is the terminal time in RK4, and the time step  $h$  is negative.  $\mathbf{P}(t)$  in  $[t_0, t_f]$  can be calculated offline.

Similarly, substituting  $\mathbf{A}$ ,  $\mathbf{B}$ ,  $R(t)$  and  $\mathbf{P}(t)$  into (28) and assuming

$$\mathbf{g}(t) = [g_1^{(x)}(t), g_2^{(x)}(t)]^T, \quad (32)$$

yields

$$\begin{aligned} \dot{g}_1^{(x)} &= t_{go}^N g_2^{(x)} p_2, \\ \dot{g}_2^{(x)} &= -g_1^{(x)} + t_{go}^N g_2^{(x)} p_3, \end{aligned} \quad (33)$$

whose terminal constraint is given by

$$g_1^{(x)}(t_f) = f_1 x_a, \quad g_2^{(x)}(t_f) = f_2 v_{ax}. \quad (34)$$

Substituting  $\mathbf{P}[t_0 : t_f]$  into (33),  $\mathbf{g}(t)$  in  $[t_0, t_f]$  can be calculated by RK4. Substituting (29) and (32) into (26), the optimal control law in X-axis becomes

$$a_x^* = t_{go}^N \left( g_2^{(x)} - p_2 x - p_3 v_x \right). \quad (35)$$

Since the solution of  $\mathbf{P}(t)$  is independent of  $\mathbf{Y}_d(t_f)$ , it is not necessary to obtain  $\mathbf{P}(t)$  repeatedly when solving the optimal

control  $a_y^*$  and  $a_z^*$  in the Y-axis and Z-axis. The solution of  $\mathbf{g}(t)$  is related to  $\mathbf{Y}_d(t_f)$  which is different in three directions so that  $\mathbf{g}(t)$  has to be solved separately. The optimal control law in the Y-axis and Z-axis are solved by the same method, and the optimal control law is obtained as

$$\begin{aligned} \mathbf{U}^* &= \begin{bmatrix} a_x^* \\ a_y^* \\ a_z^* \end{bmatrix} = t_{go}^N \begin{bmatrix} g_2^{(x)} - p_2 x - p_3 v_x \\ g_2^{(y)} - p_2 y - p_3 v_y \\ g_2^{(z)} - p_2 z - p_3 v_z \end{bmatrix} \\ &= t_{go}^N [\mathbf{G} + p_2 (\mathbf{r}_t - \mathbf{r}_u) + p_3 (\mathbf{v}_t - \mathbf{v}_u)], \end{aligned} \quad (36)$$

where  $\mathbf{G} = \left( g_2^{(x)}, g_2^{(y)}, g_2^{(z)} \right)^T$  are adjoint vectors in X-axis, Y-axis and Z-axis, respectively. Substituting (36) into (13), the optimal control law for a single UAV becomes

$$\mathbf{a}_u = \mathbf{a}_t + t_{go}^N [\mathbf{G} + p_2 (\mathbf{r}_t - \mathbf{r}_u) + p_3 (\mathbf{v}_t - \mathbf{v}_u)]. \quad (37)$$

UAV's control input is calculated by substituting target's real-time position  $\mathbf{r}_t$ , velocity  $\mathbf{v}_t$  and acceleration  $\mathbf{a}_t$  into (37). In other words, UAV's control input is only relative to target's current state, rather than past or future motion. Therefore, the state of the target is changing and known in real time, but the future state of the target is uncertain.

### B. TIME-COORDINATED CONTROL FOR UAV SWARM

Compared with attacking ground target with a single UAV, the advantage of UAV swarm is that there are massive emergences of attack effectiveness, with the time-coordinated capabilities. Therefore, the arrival time of each UAV should be limited, according to different time-coordinated strategies. The constrain of each arrival time has the form of

$$\Gamma(t_{f,1}, t_{f,2}, \dots, t_{f,N}) = 0, \quad (38)$$

where  $\Gamma(\cdot)$  is time-coordinated function,  $t_{f,i}$  is the arrival time of  $i$ th UAV. When adopting the strategy of interval arrival,  $\Gamma(\cdot)$  can be expressed as

$$t_{f,i} - t_{f,j} = \Delta t_{ij}, \quad \forall i, j \in [1, n], \quad (39)$$

where  $\Delta t_{ij}$  is the interval time between  $i$ th UAV and  $j$ th UAV. Specially, when  $\Delta t_{ij} = 0$ , the interval time is equal to zero. In other words, all UAVs arrive at the DAP simultaneously, and  $\Gamma(\cdot)$  becomes

$$t_{f,i} = t_f, \quad \forall i \in [1, n], \quad (40)$$

where  $t_f$  is the simultaneous arrival time. Similarly, more complex time-coordinated strategies can be expressed by constructing different time-coordinated function. Such as a strategy of simultaneous arrival within one group and interval arrival between groups,  $\Gamma(\cdot)$  becomes

$$\begin{cases} t_{f,i} = t_f^{(k)}, \\ t_f^{(p)} - t_f^{(q)} = \Delta t_{pq}, \end{cases} \quad \forall i \in \Omega_k, \quad \forall p, q \in [1, n], \quad (41)$$

where  $\Omega_k$  is the set of UAV labels of the  $k$ th attack group,  $t_f^{(k)}$  is the simultaneous arrival time of  $\Omega_k$ ,  $\Delta t_{pq}$  is the time interval between the  $p$ th group and  $q$ th group. In section IV,

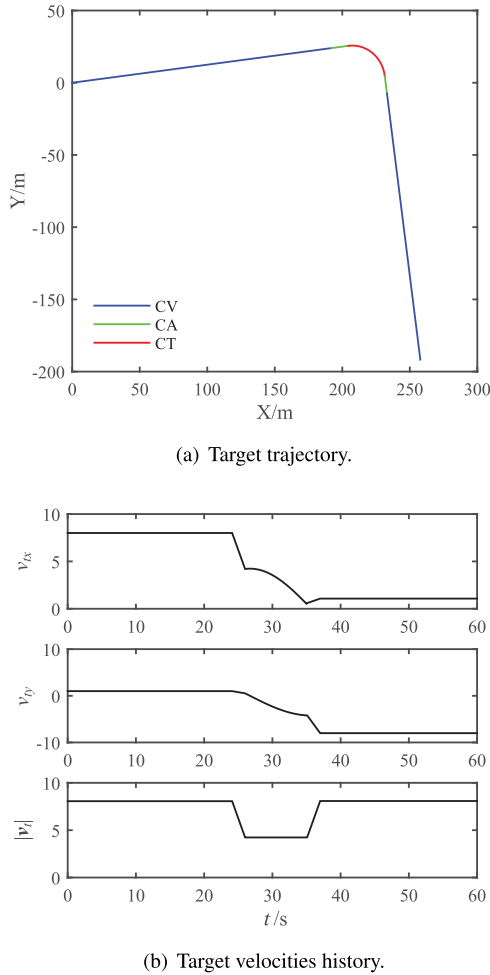


FIGURE 5. Trajectory and velocities of target in simulation.

the time-coordinated strategies mentioned above are applied to verify the effectiveness of proposed time-coordinated control law.

On the basis of the control law proposed in this paper, the real-time communication in the swarm is not required, but the communication of coordinated variables is necessary at the initial time. Before the attack, all UAVs in UAV swarm should coordinate their arrival time  $t_{f,i}$  and the DAP  $X_{DAP,i}$  according to the requirements of mission. For  $i$ th UAV in the swarm, the parameters  $p_{2,i}$ ,  $p_{3,i}$  and the adjoint vector  $G_i$  in  $[t_0 : t_f]$  can be obtained based on the predefined  $t_{f,i}$  and  $X_{DAP,i}$ . The time-coordinated control law for  $i$ th UAV is

$$a_{ui} = a_t + (t_{f,i} - t)^N [G_i + p_{2,i} (r_t - r_{ui}) + p_{3,i} (v_t - v_{ui})]. \quad (42)$$

The actual controls are computed by substituting (42) into (5).

**Remark 2:** There is no formal difference of control law between a single UAV and UAV swarm, but the different parameters are adopted for each UAV. The position  $r_{ui}$  and velocity  $v_{ui}$  of each UAV are different in real time and the terminal arrival time  $t_{f,i}$  may be various. The different terminal

arrival time  $t_{f,i}$  and desired arrival position  $Y_d(t_{f,i})$  cause that the parameters  $p_{2,i}$ ,  $p_{3,i}$  and  $G_i$  are distinct for each UAV.

#### IV. SIMULATION ANALYSIS

In this section, we investigate the performance of the proposed time-coordinated strategy given in (41) for the control law (42). The drag for each UAV in this paper is introduced by [29]

$$D_g = \frac{1}{2} \rho (V_g - V_\omega)^2 S C_{D0} + \frac{2k_d k_n^2 n_g^2 m^2}{\rho (V_g - V_\omega)^2 S}, \quad (43)$$

where  $V_\omega$  is the velocity of wind. The UAV's wing area and weight are assumed to be  $S = 4m^2$  and  $m = 20kg$ , respectively. Other parameters in the model are: atmospheric density  $\rho = 1.225kg/m^3$ , zero-lift drag coefficient  $C_{D0} = 0.02$ , induced drag coefficient  $k_d = 0.1$ , load-factor effectiveness  $k_n = 1$ , gravitational acceleration  $g_a = 9.81m/s^2$ . The influence of wind is negligible and the wind speed is assumed to be zero,  $V_\omega = 0$ . The constraints on the actual control variables are  $T_h \leq 200N$ ,  $-1.5 \leq n_g \leq 2.0$  and  $-50^\circ \leq \phi \leq 50^\circ$ .

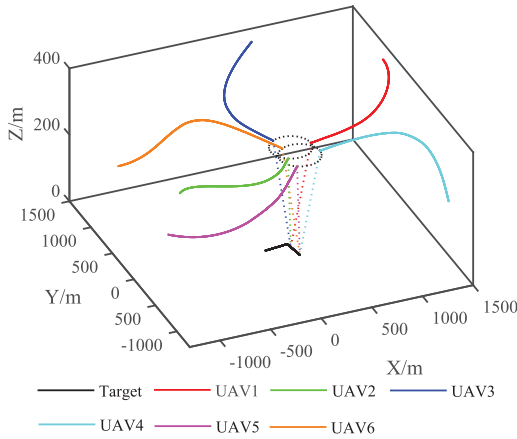
The ground-moving target is assumed to be a vehicle running on roads, and its altitude is a constant, i.e.  $z_t = 0$ . Target's initial state is

$$X_t(0) = (0m, 8m/s, 0m, 1m/s)^T. \quad (44)$$

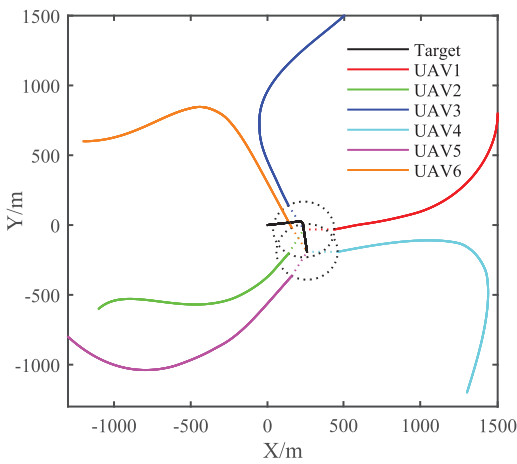
In this simulation, the movement of target is based on the CV, CA and CT models given in (9-11). Assume that the target moves as: constant linear motion in 0 – 24s, uniformly decelerated motion with deceleration of  $(-2, -0.25) m/s^2$  in 24 – 26s, coordinate right turn motion within 26 – 35s, uniformly accelerated motion with acceleration of  $(0.25, -2) m/s^2$  in 35 – 37s, constant linear motion in 37 – 60s. The trajectory and velocity are shown in Fig. 5(a) and Fig. 5(b).

Note that each UAV can only obtain the state of target in real time, and the motion in the whole process is unknown. A time-coordinated attack strategy, simultaneous arrival within a group and interval arrival between groups, is adopted here to verify the effectiveness of the proposed control law. In this scenario, the UAV swarm including 6 UAVs, which is divided into two subgroups, is assigned to attack a ground-moving target. The first subgroup is composed of UAV1, UAV2 and UAV3, and the second is UAV4, UAV5 and UAV6. A circle with a radius of 200 meters is set as an attack circle at a height of 300 meters above the target, and three points on the attack circle from different directions are chosen as three DAPs. The initial position, initial velocity, DAP and arrival time of all UAVs are given in Table 1.

In addition, parameters of DAP on Z-axis for all UAVs is  $z_a = 300m$  and  $v_{az} = 0m/s$ . The time step is taken  $T = 0.1s$ , and the associated weights in control law are set to  $f_1 = 2$ ,  $f_2 = 1$  and  $N = 1$ . The simulation results of the UAV swarm under the proposed time-coordinated control law (42) are shown in Figs. 6-9. The simulation results of UAV1-3 are limited in 0 – 40s and UAV4-6 in 0 – 60s. Fig. 6(a) and



(a) 3-D trajectories of UAV swarm time-coordinated attack.



(b) Top view of 3-D trajectories.

FIGURE 6. Trajectories of UAV swarm time-coordinated attack.

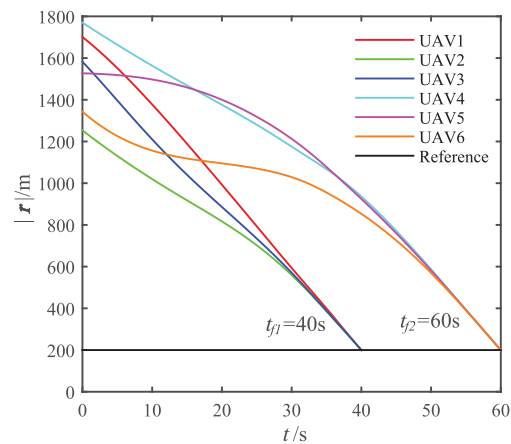
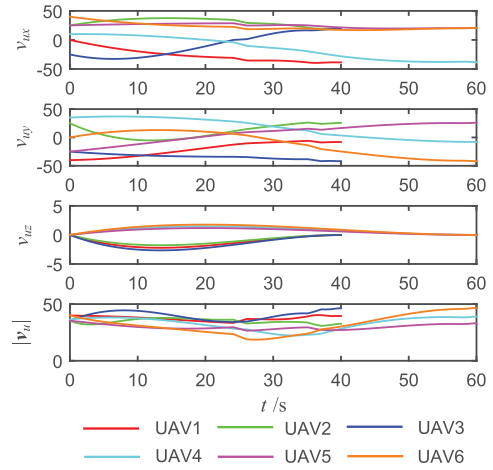


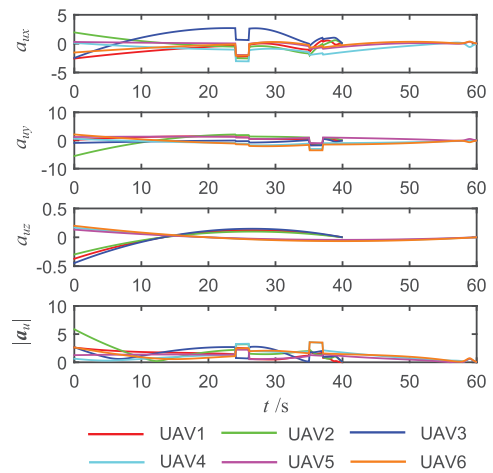
FIGURE 7. Relative distances history between UAVs and target.

Fig. 6(b) show the 3-D trajectories of the UAV swarm and top view of the trajectory, respectively.

As can be seen from Fig. 6, UAV1, UAV2 and UAV3 reached their DAPs simultaneously with the expected



(a) Time histories of UAVs' velocities.



(b) Time histories of UAVs' accelerations.

FIGURE 8. Velocity and accelerations of UAVs in simulation.

relative speed, achieving the effect of time-coordinated attack. After a certain interval time, UAV4, UAV5 and UAV6 also reached their DAPs simultaneously. The flight trajectories of all UAVs are smooth and accord with the actual situation. The time histories of the relative distances between UAVs and target are given in Fig. 7.

As shown in Fig. 7, the terminal relative distances between UAVs and target converge to reference at  $t = 40s$  and  $t = 60s$ , respectively. This is achieved by optimizing the terminal error term in the (20). Figs. 8-9 present the history of the UAVs' velocity, acceleration and actual controls.

As shown in Fig. 8(b), the accelerations of UAVs change dramatically during 24–26s and 35–37s, which is influenced by the acceleration and deceleration of the target. Furthermore, the control input of UAVs converges to zero at and for the first subgroup and the second subgroup, respectively. Fig. 9 illustrates the time history of thrust, g-load, banking angle and flight path angle, respectively. The first three figures in Fig. 9 demonstrate the actual controls which are



TABLE 1. Initial State and Terminal Expected State of UAV Swarm.

Label	$r_u(0), m$			$v_u(0), m/s$			$X_{DAP}, m, m/s$				$t_f, s$
	$x_u$	$y_u$	$z_u$	$v_{ux}$	$v_{uy}$	$v_{uz}$	$x_a$	$y_a$	$v_{ax}$	$v_{ay}$	
1	1500	800	350	0	-40	0	200	0	-40	0	40
2	-1100	-600	340	25	25	0	-100	-173.2	20	34.6	40
3	500	1500	360	-25	-25	0	-100	173.2	20	-34.6	40
4	1300	-1200	250	10	35	0	200	0	-40	0	60
5	-1300	-800	260	25	-25	0	-100	-173.2	20	34.6	60
6	-1200	600	240	40	0	0	-100	173.2	20	-34.6	60

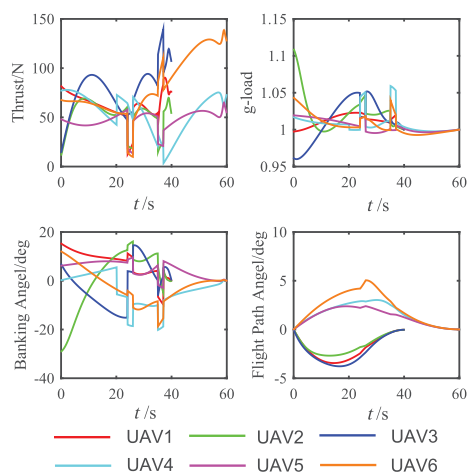


FIGURE 9. Time histories of UAVs' actual controls.

computed using (5). Obviously, all of the actual controls are within the prescribed constraints.

V. CONCLUSION

Time-coordinated control problems for UAV swarm cooperative attack are investigated in this paper, where the target is moving on the ground. Relative motion between UAV and ground-moving target are considered as a finite-time time-varying tracking system problem. Proposed control law for a single UAV is obtained by linear quadratic optimal control theory, which can guide the UAV to the desired attack positions with the specified terminal time and relative velocity. Time-coordinated function is proposed to model time-coordinated strategies, and different functions are constructed to implement various strategies. On the basis of proposed control law for a single UAV, the control law for UAV swarm is obtained by substituting the parameters of each UAV. Numerical simulations show that the proposed control law can steer the UAV to arrive at the desired attack positions and effectively realize the time-coordinated strategies. But with the acceleration or turning of the target, the actual controls extreme fluctuate. There are still a number of issues need to be further investigated and coordinated control for UAV swarm in various missions are currently under investigation. Another thing needs to be addressed in the future is that other constraints such as control saturation, target's moving speed,

measurement error, time delay and collision avoidance should be taken into consideration.

ACKNOWLEDGMENT

The authors would like to thank the editors and reviewers for their suggestions, which are of great value to for revising and improving our paper, as well as the important guiding significance to our researches.

REFERENCES

- [1] L. Hu, P. Bai, X. Liang, J. Zhang, and W. Wang, "Solution and optimization of aircraft swarm cooperating anti-stealth formation configuration," *IEEE Access*, vol. 6, pp. 71485–71496, 2019.
- [2] M. Suresh and D. Ghose, "UAV grouping and coordination tactics for ground attack missions," *IEEE Trans. Aerosp. Electron. Syst.*, vol. 48, no. 1, pp. 673–692, Jan. 2012.
- [3] Z. Kan, S. S. Mehta, E. L. Pasilio, J. W. Curtis, and W. E. Dixon, "Balanced containment control and cooperative timing of a multi-agent system," in *Proc. Amer. Control Conf.*, Jun. 2014, pp. 281–286.
- [4] H. Zhang, T. Feng, G.-H. Yang, and H. Liang, "Distributed cooperative optimal control for multiagent systems on directed graphs: An inverse optimal approach," *IEEE Trans. Cybern.*, vol. 45, no. 7, pp. 1315–1326, Jul. 2015.
- [5] H. Zhang, J. Zhang, G.-H. Yang, and Y. Luo, "Leader-based optimal coordination control for the consensus problem of multiagent differential games via fuzzy adaptive dynamic programming," *IEEE Trans. Fuzzy Syst.*, vol. 23, no. 1, pp. 152–163, Feb. 2015.
- [6] P. F. J. Lermusiaux, T. Lolla, P. J. Haley, Jr., K. Yigit, M. P. Ueckermann, T. Sondergaard, and W. G. Leslie, "Science of autonomy: Time-optimal path planning and adaptive sampling for swarms of ocean vehicles," in *Springer Handbook of Ocean Engineering*. Berlin, Germany: Springer, 2016, pp. 481–498.
- [7] E. Xargay, V. Dobrokhodov, I. Kaminer, A. M. Pascoal, N. Hovakimyan, and C. Cao, "Time-critical cooperative control of multiple autonomous vehicles: Robust distributed strategies for path-following control and time-coordination over dynamic communications networks," *IEEE Control Syst. Mag.*, vol. 32, no. 5, pp. 49–73, Oct. 2012.
- [8] T. W. McLain and R. W. Beard, "Coordination variables, coordination functions, and cooperative timing missions," *J. Guid. Control Dyn.*, vol. 28, no. 1, pp. 150–161, 2005.
- [9] C.-K. Ryoo, Y.-H. Kim, and M.-J. Tahk, "Optimal UAV formation guidance laws with timing constraint," *Int. J. Syst. Sci.*, vol. 37, no. 6, pp. 415–427, 2006.
- [10] B.-M. Min, C.-K. Ryoo, and M.-J. Tahk, "Guidance law for formation flight with terminal time constraint," *Trans. Jpn. Soc. Aeronaut. Space Sci.*, vol. 57, pp. 40–48, Jan. 2014.
- [11] I.-S. Jeon, J.-I. Lee, and M.-J. Tahk, "Impact-time-control guidance law for anti-ship missiles," *IEEE Trans. Control Syst. Technol.*, vol. 14, no. 2, pp. 260–266, Mar. 2006.
- [12] Z. Shiyu, Z. Rui, W. Chen, and D. Quanxin, "Design of time-constrained guidance laws via virtual leader approach," *Chin. J. Aeronaut.*, vol. 23, no. 1, pp. 103–108, 2010.
- [13] G. A. Harrison, "Hybrid guidance law for approach angle and time-of-arrival control," *J. Guid., Control, Dyn.*, vol. 35, no. 4, pp. 1104–1114, 2012.

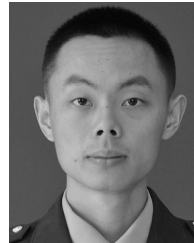
- [14] Z. Hu, M. Zhao, and M. Yao, "Cooperative attack path planning for unmanned air vehicles swarm based on grid model and bi-level programming," *J. Inf. Comput. Sci.*, vol. 8, no. 4, pp. 671–679, 2011.
- [15] D. B. Kingston, W. Ren, and R. W. Beard, "Consensus algorithms are input-to-state stable," in *Proc. Conf. Amer. Control Conf.*, vol. 3, Jun. 2005, pp. 1686–1690.
- [16] F. Yan, X. Zhu, Z. Zhou, and Y. Tang, "Heterogeneous multi-unmanned aerial vehicle task planning: Simultaneous attacks on targets using the pythagorean hodograph curve," *Proc. Inst. Mech. Eng., G, J. Aerosp. Eng.*, pp. 1–15, Feb. 2019. doi: [10.1177/0954410019829368](https://doi.org/10.1177/0954410019829368).
- [17] S. G. Manyam, D. W. Casbeer, and S. Manickam, "Optimizing multiple UAV cooperative ground attack missions," in *Proc. Int. Conf. Unmanned Aircr. Syst. (ICUAS)*, Jun. 2017, pp. 1572–1578.
- [18] M. Zhang and H. H. T. Liu, "Cooperative tracking a moving target using multiple fixed-wing UAVs," *J. Intell. Robot. Syst.*, vol. 81, nos. 3–4, pp. 505–529, 2016.
- [19] P. Yao, H. Wang, and Z. Su, "Cooperative path planning with applications to target tracking and obstacle avoidance for multi-UAVs," *Aerosp. Sci. Technol.*, vol. 54, no. 1, pp. 10–22, 2016.
- [20] H. Zhang, Q. Wei, and Y. Luo, "A novel infinite-time optimal tracking control scheme for a class of discrete-time nonlinear systems via the greedy HDP iteration algorithm," *IEEE Trans. Syst., Man, Cybern. B, Cybern.*, vol. 38, no. 4, pp. 937–942, Aug. 2008.
- [21] J. Wang and M. Xin, "Integrated optimal formation control of multiple unmanned aerial vehicles," *IEEE Trans. Control Syst. Technol.*, vol. 21, no. 5, pp. 1731–1744, Sep. 2013.
- [22] N. Rong, Z. Wang, and H. Zhang, "Finite-time stabilization for discontinuous interconnected delayed systems via interval type-2 T-S fuzzy model approach," *IEEE Trans. Fuzzy Syst.*, vol. 27, no. 2, pp. 249–261, Feb. 2019.
- [23] N. Rong and Z. Wang, "Fixed-time stabilization for IT2 T-S fuzzy interconnected systems via event-triggered mechanism: An exponential gain method," *IEEE Trans. Fuzzy Syst.*, to be published.
- [24] P. K. A. Menon, "Short-range nonlinear feedback strategies for aircraft pursuit-evasion," *J. Guid. Control Dyn.*, vol. 12, no. 1, pp. 27–32, 1989.
- [25] P. K. Menon, G. D. Sweriduk, and B. Sridhar, "Optimal strategies for free-flight air traffic conflict resolution," *J. Guid., Control, Dyn.*, vol. 22, no. 2, pp. 202–211, 1997.
- [26] X. R. Li and V. P. Jilkov, "Survey of maneuvering target tracking. Part I. Dynamic models," *IEEE Trans. Aerosp. Electron. Syst.*, vol. 39, no. 4, pp. 1333–1364, Oct. 2003.
- [27] H. Cho, C.-K. Ryoo, A. Tsourdos, and B. White, "Optimal impact angle control guidance law based on linearization about collision triangle," *J. Guid. Control Dyn.*, vol. 37, no. 3, pp. 958–964, 2014.
- [28] A. E. Bryson, Y.-C. Ho, and G. M. Siouris, "Applied optimal control: Optimization, estimation, and control," *IEEE Trans. Syst., Man, Cybern.*, vol. 9, no. 6, pp. 366–367, Jun. 1979.
- [29] Y. Xu, "Nonlinear robust stochastic control for unmanned aerial vehicles," in *Proc. Amer. Control Conf.*, Jun. 2009, pp. 2819–2824.



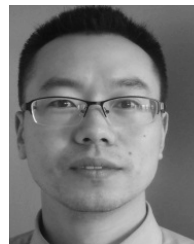
**YUEQI HOU** was born in 1995. He received the B.S. degree from the Air Traffic Control and Navigation College, Air Force Engineering University, Xi'an, China, in 2017, where he is currently pursuing the M.S. degree in control science and engineering. His research interests include intelligent decision and cooperative control of aircraft swarm.



**XIAOLONG LIANG** was born in 1981. He received the master's degree in operational research and cybernetics and the Ph.D. degree in armament science and technology from Air Force Engineering University. He is now a professor of the Air Traffic Control and Navigation College, Air Force Engineering University. He has published more than 50 journal papers and finished more than 20 projects. His research interests include aircraft swarm technology, airspace management intelligence, and intelligent aviation system. He is a major of several national scientific research projects.



**LYULONG HE** was born in 1990. He received the B.S. degree from the Nanjing University of Aeronautics and Astronautics, Nanjing, China, in 2013, and the M.S. degree from Air Force Engineering University, Xi'an, China, in 2015, where he is currently pursuing the Ph.D. degree. He is also an Assistant Engineer with the Shaanxi Province Laboratory of Meta-Synthesis for Electronic and Information System. His current research interest includes consensus and formation control of multi-agent systems with applications to aircraft swarm formation flying.



**JIAQIANG ZHANG** was born in 1984. He received the M.S. degree in weapon system and application engineering and the Ph.D. degree in armament science and technology from the School of Aeronautics and Astronautics Engineering, Air Force Engineering University, in 2009 and 2012, respectively, where he is currently a Lecturer with the School of Air Traffic Control and Navigation College. He has published more than 20 journal papers and finished more than ten projects. His research interests include aircraft swarm technology and airspace management intelligence.

• • •